Letters

Accurate FCS Model Predictive Current Control Technique for Surface-Mounted PMSMs at Low Control Frequency

Chao Gong, *Student Member, IEEE*, Yihua Hu, *Senior Member, IEEE*, Mingyao Ma, *Member, IEEE*, Liming Yan, Jinglin Liu, *Member, IEEE*, and Huiqing Wen, *Senior Member, IEEE*

***Abstract*—In order to enhance the control performance of the surface-mounted permanent magnet synchronous machines (PMSM) working under the low frequency situations, this letter innovatively proposes an accurate finite control set (FCS) model predictive current control (MPCC) method. First, a novel predicting plant model in the continuous-time domain based on the numerical solutions of the PMSM state-space model (differential equations) is developed. Without using the linear discretization implementation, the influence of the low control frequency can be eliminated completely. Besides, a brand-new calculation delay compensation method based on delay time prediction and current precompensation is designed for the proposed FCS–MPCC strategy. Finally, experiments are conducted on a PMSM test bench with the control frequencies of 2 and 1 kHz to comprehensively verify the proposed algorithms.**

***Index Terms*—Delay compensation, low control frequency (LCF), model predictive current control (MPCC), permanent magnet synchronous machine (PMSM).**

I. Introduction

In industry, surface-mounted permanent magnet synchronous machines (PMSM) have been widely adopted thanks to its high torque and power density and compact structure [1]–[3]. Among the high-performance PMSM control strategies, because the finite control set (FCS) model predictive current control (MPCC) strategy has high dynamics and simple structure, it draws increasing attention from both the scholars and engineers [4]. Nowadays, most of the FCS–MPCC methods are achieved relying on the forward Euler discretization-based plant model of the machine, and usually, the discretization time step equals the sampling (control) cycle [5]. Practically, in order to reduce the torque and current ripples of the drive system, the control frequency should stand at a pretty high position (e.g., 10 kHz). As is shown in paper [6], the control performance of an FCS–MPCC controller is as remarkable as that of the space vector pulsewidth modulation based field-oriented control methods as the switching/control frequency is high. Whereas, it is widely acknowledged that the high switching/control frequency will generate quantities of loss and heat in the power devices, lowering the efficiency and reliability of the whole system. Considering this issue, many up-to-date researches have focused on the low control frequency (LCF) drives [7], [8]. However, the control performance will witness a marked degradation (e.g., higher torque and current ripples) when the system works at the LCF. As for the traditional FCS–MPCC strategy, one crucial reason for this phenomenon is that the discretization process is inaccurate. In detail, as shown in Fig. 1, the Euler discretization approach implies that the system state value i_p will shift in a linear trend when a particular candidate voltage vector is applied in each control period, while this default assumption does not conform to the real situations because of the nonlinear property of the system (real state is i_r). When the control period increases, the accuracy of the one-step prediction results will decline greatly. Namely, distinct errors between the predicted values and the real ones will emerge as the control frequency becomes low. For example, in Fig. 1, when the control period increases from T_1 to T_2, the current error grows from $\triangle i_1(k+1)$ to $\triangle i_2(k+1)$. This will inevitably influence the optimal

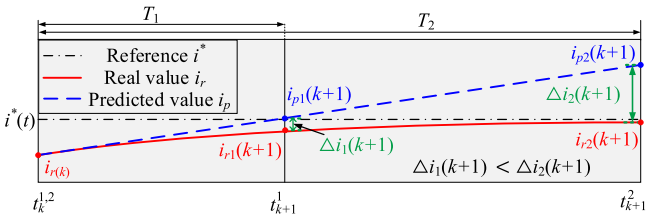

Fig. 1. Prediction process of traditional FCS–MPCC method.

Manuscript received August 28, 2019; revised September 30, 2019, November 3, 2019, and November 11, 2019; accepted November 12, 2019. Date of publication November 14, 2019; date of current version February 20, 2020. *(Corresponding author: Mingyao Ma.)*

C. Gong and Y. Hu are with the Department of Electrical Engineering and Electronics, University of Liverpool, Liverpool L69 3GJ, U.K. (e-mail: 1452101806@qq.com; y.hu35@liverpool.ac.uk).

M. Ma is with the School of Electrical Engineering and Automation, Hefei University of Technology, Hefei 230009, China (e-mail: miyama@hfut.edu.cn).

L. Yan is with the School of Automobile, Chang'an University, Xi'an 710064, China (e-mail: ylm@chd.edu.cn).

J. Liu is with the School of Automation, Northwestern Polytechnical University, Xi'an 710129, China, and also with the Shaanxi Key Laboratory of Small and Special Electrical Machine and Drive Technology, Northwestern Polytechnical University, Xi'an 710129, China (e-mail: jinglinl@nwpu.edu.cn).

H. Wen is with the Department of Electrical and Electronic Engineering, Xi'an Jiaotong-Liverpool University, Suzhou 215123, China (e-mail: Huiqing.Wen@xjtlu.edu.cn).

Color versions of one or more of the figures in this article are available online at http://ieeexplore.ieee.org.

Digital Object Identifier 10.1109/TPEL.2019.2953787

switching state selection process of an FCS–MPCC controller, and further degrade its control performance.

Another common problem of the FCS–MPCC strategy for PMSM drives is that the quantities of calculations have to be executed during the optimal control voltage process, resulting in that the calculation time is long [9], [10]. The time delay between the state measurement and actuation would lead to inaccurate selection of the control voltage and further deteriorate the system performance if it is not considered, lessening the effect of optimal control. Many scholars have addressed the time delay issue of FCS–MPC. For the traditional linear discretization-based FCS–MPCC, the most commonly used delay compensation method is the two-step prediction (TSP) strategy that uses the machine model shifted one step forward to calculate the manipulated voltages [11], [12]. These indicate that tackling the calculation problem is crucial for improving the control performance of an FCS–MPCC controller and it is highly required to develop effective delay compensation approaches for any newly developed FCS–MPCC methods.

In order to overcome the drawbacks of the traditional discretization method and increase the control performance for the LCF situations, a novel FCS–MPCC algorithm by using an innovative numerical solution based predicting plant model (PPM) is developed in this letter. Without using the linear discretization, the traditional calculation delay compensation method based on TSP technique will no longer be totally applicable. On this ground, a brand-new delay handling approach that includes two sequential procedures (dual-sampling-technique-based delay time estimation and current precompensation) is discussed. The experimental results verify the effectiveness of the proposed strategies.

II. Numerical Solution Based Predicting Plant

In terms of FCS–MPCC, the targeting control objectives are the *d*-, *q*-axis currents, so only the electrical equations are required for prediction. The electrical properties of a surface-mounted PMSM in the rotating reference frame can be illustrated as follows:

$$\begin{cases} \frac{\mathrm{d}i_d}{\mathrm{d}t} = -\frac{R_s}{L} i_d + p\omega_m i_q + \frac{u_d}{L} \\ \frac{\mathrm{d}i_q}{\mathrm{d}t} = -p\omega_m i_d - \frac{R_s}{L} i_q + \frac{u_q}{L} - \frac{\Psi_f}{L} p\omega_m \end{cases} \tag{1}$$

where ω_m is the rotor mechanical angular speed. i_d, i_q are the *dq*-axis currents. u_d, u_q are *dq*-axis control voltages. L is the stator inductance. R_s is the stator winding resistance. p and Ψ_f represent the number of pole pairs and the flux linkage, respectively. Instead of discretizing the machine model with a linear method, a novel PPM based on the numerical solutions of (1) will be established. To solve the differential equations, the solutions can be expressed as follows:

$$\begin{cases} i_d(t) = \frac{m}{c} + [\frac{y}{c}\sin(p\omega_m t) + \frac{z}{c}\cos(p\omega_m t)] \cdot \exp\left(-\frac{R_s t}{L}\right) \\ i_q(t) = -\frac{n}{c} + [\frac{y}{c}\cos(p\omega_m t) - \frac{z}{c}\sin(p\omega_m t)] \cdot \exp\left(-\frac{R_s t}{L}\right) \end{cases} \tag{2}$$

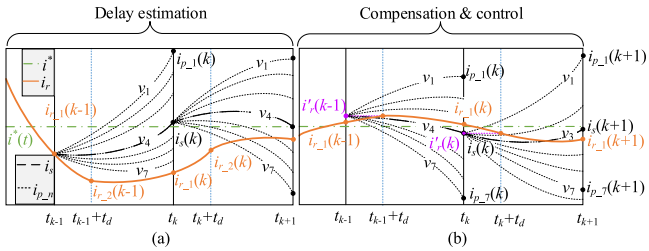

Fig. 2. Proposed delay compensation strategy. (a) Delay effect and delay prediction. (b) Compensation and control process.

where

$$\begin{cases} m = -p^2 L \Psi_f \omega_m + pL\omega_m u_q + R_s u_d \\ n = pR_s \Psi_f \omega_m + pL\omega_m u_d - R_s u_q \\ c = p^2 L^2 {\omega_m}^2 + {R_s}^2 \\ y = c \cdot i_q(t_0) + n \\ z = c \cdot i_d(t_0) - m \end{cases} \tag{3}$$

where $i_d(t_0)$ and $i_q(t_0)$ are the boundary condition. During prediction, let $i_d(t_0)$ and $i_q(t_0)$ equal the instantaneous sampling values at the start of each control period. Then, the states at the next instant, $i_d(t_0 + T)$ and $i_q(t_0 + T)$, can be calculated by setting the time *t* as the control period *T*. Obviously, the proposed PPM can reflect the continuous (real) current shift trend in a machine, being able to obtain the more accurate prediction results in comparison with the traditional strategy, especially in the LCF applications.

Before leaving the PPM, it should be noticed that the numerical solution-based method is more complex due to the operations of the exponential and trigonometric functions compared to the traditional FCS–MPCC method [5], resulting in larger computation burden. In Chapter III, the calculation delay caused by the proposed algorithms will be compensated using a brand-new technique.

III. Novel Calculation Delay Compensation

The calculation delay effect is illustrated in Fig. 2(a), where i^* and i_r are the trajectory of reference current and real current, respectively, i_{p_n} is the estimated current corresponding to the different voltage vectors and i_s is the estimated current when the calculated voltage vector is applied. Because there are fixed algorithms to be implemented in each control period for a PMSM drive, the calculation time t_d can be assumed to be identical for each cycle. It can be noted that between t_{k-1} and t_k, the voltage vector v_4 is the optimal manipulated voltage if the calculation delay is ignored. However, as a result of t_d, the selected switching state is applied with delay at $t_{k-1} + t_d$, leading to that the current locus cannot be controlled as expected and a large deviation occurs after a control period of *T*. Inevitably, this phenomenon will deteriorate the control performance of the PMSM system.

Considering the computation delay problem, Fig. 2 illustrates a specially designed delay compensation strategy for the proposed numerical solution based FCS–MPCC scheme. It consists of two sequential parts: online delay time prediction and implementation of current precompensation and control.

A. Delay Prediction

In order to estimate the delay time, the proposed FCS–MPCC algorithm based on the new predicting model without delay compensation should be conducted on the PMSM at first [see Fig. 2(a)]. It can be noted that different from the traditional single sampling technique, sampling is implemented twice in each control period, one of which is still at the beginning of a period, and the other is after voltage selection but before switching state actuation. At length, the sampling currents over t_{k-1}–t_k and t_k–t_{k+1} are $i_{r\_1(k-1)}, i_{r\_2(k-1)}$ and $i_{r\_1(k)}, i_{r\_2(k)}$, respectively. Besides, the control voltage within t_d should be the one applied in the last step. Between t_k and $t_k + t_d$, according to the d-axis predicting plant, the time delay equals the solution of (4)

$$i_{r\_2}(k) = \frac{m}{c} + \left[\frac{y}{c}\sin(p\omega_m t_d) + \frac{z}{c}\cos(p\omega_m t_d)\right] \cdot \exp\left(-\frac{R_s t_d}{L}\right). \tag{4}$$

Definitely, it is tedious to solve this equation. First, because t_d is tiny, the variation of $\sin(p\omega_m t_d)$ is much larger than $\cos(p\omega_m t_d)$ within t_d. It is appropriate to approximate the sine function to $p\omega_m t_d$ while the cosine function to 1 according to the theorem of equivalent infinitesimal replacement. Meanwhile, $\exp(-\frac{R_s t_d}{L})$ is equivalent to $1 - \frac{R_s t_d}{L}$. Then, (4) can be simplified as follows:

$$i_{r\_2}(k) = -\frac{yR_s}{cL} \cdot {t_d}^2 + \left(\frac{y}{c} - \frac{zR_s}{cL}\right) \cdot t_d + \frac{m+z}{c}. \tag{5}$$

And t_d can be derived as follows:

$$t_d = \frac{yL - zR_s + \sqrt{\begin{array}{r}-4LR_s cy i_{r\_2}(k) + 4LR_s my \\ +2LR_s zy + {R_s}^2 z^2\end{array}}}{2yR_s}. \tag{6}$$

Practically, in order to increase the accuracy of delay estimation, (6) can be executed repetitiously in multiple (e.g., $N = 15$) cycles, and then, the average value would be adopted as the required result.

B. Implementation of Current Precompensation and Control

After obtaining t_d, the dual-sampling technique is unnecessarily adopted for the compensation and control process [as in Fig. 2(b)] any longer. As is illustrated in Fig. 3, the proposed FCS–MPCC algorithm based on the accurate plant model and compensation includes following six stages at the kth instant.

1) State measurement: Detect the real-time phase currents, rotor position $\theta(k)$ and speed $\omega_m(k)$ and transform the three phase currents i_a, i_b, and i_c to the d-, q-axis currents $i_d(k)$ and $i_q(k)$ [denoting $i_{r\_1}(k)$) in Fig. 2(b)] according to $\theta(k)$.
2) Precompensation: Let the measured currents equal the boundary condition and predict the currents $i'_d(k)$ and $i'_q(k)$ [denoting $i'_r(k)$ in Fig. 2(b)] in t_d following the (2) and (3) using the control voltage in the previous cycle, where $i'_r(k)$ represents the compensated current.
3) Prediction: Let the compensated currents $i'_d(k)$ and $i'_q(k)$ equal the boundary condition and substitute them together with $\omega_m(k)$ into the PPM to estimate the future current states $i_d(t_0 + T)$ and $i_q(t_0 + T)$ for all the candidate manipulated voltage vectors.
4) Evaluation: Substitute all the predicted currents one by one into a cost function and select the voltage vector that minimizes the cost function.

$$g = (i_d{}^* - i_d(t_0 + T))^2 + (i_q{}^* - i_q(t_0 + T))^2 \tag{7}$$

where i_d^*, i_q^* are the d-, q-axis reference currents, respectively.
5) Storage: Store the selected optimal voltage vector which will be used in stage 2 in the next control period.
6) Switching state application: Single out the corresponding switching state according to the best voltage vector and apply it to the system.

Theoretically, the real current at $t_{k+1} + t_d$ will reach $i_{s(k+1)}$, indicating that the proposed method obeys the optimum control principle.

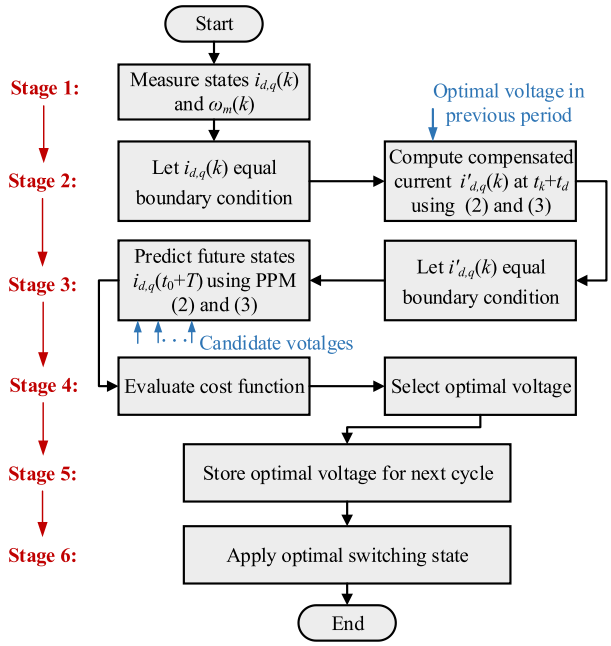

Fig. 3. Flow diagram for the implementation of the proposed FCS–MPCC method.

IV. Verifications

Experiments are carried out to verify the proposed FCS–MPCC strategy on a surface-mounted PMSM drive whose parameters are: bus voltage $U_{\rm dc} = 60$ V, rated speed

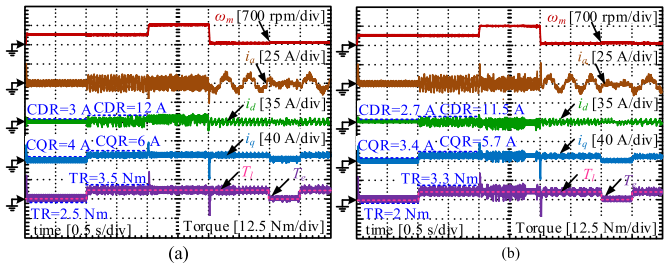

Fig. 4. Experimental results at control frequency of 2 kHz. (a) FCS–MPCC based on Euler discretization method. (b) FCS–MPCC based on proposed prediction plant without delay compensation.

$\omega_{\text{rated}} = 700$ r/min and rated load torque $T_{\text{rated}} = 5$ N·m, phase resistance $R_s = 0.6383\ \Omega$, flux linkage $\psi_f = 0.085$ Wb, inductance $L = 2$ mH, the number of pole pairs $p = 4$, viscous coefficient $B = 0.0035$, rotor inertia $J = 0.013$ kg·m^2. The algorithms are implemented on a DSP TMS320X28335 control board. For the sake of comprehensive analysis, the system is tested at the control frequencies of 2 and 1 kHz, respectively. Finally, it needs to be mentioned that in each control period, the codes of both the novel and conventional FCS–MPCC methods are executed once.

A. Test Results at 2 kHz

On the one hand, in order to compare the control performance of the traditional discretization method and the proposed strategy, both the two algorithms are verified first without using any compensation techniques. The experimental setup is as follows: the machine speeds up from standstill to 350 r/min (medium speed) between 0 and 1 s, after which it stabilizes in the next 1 s. At 1 s, the rated load is imposed on the shaft suddenly, and from 2 s, the reference speed is set as 700 r/min (high speed). At 3 s, the speed decreases to 50 r/min (ultra-low speed), after which the speed will remain at this level until 5 s. Moreover, the load is suddenly removed and then applied again at 4 and 4.5 s respectively. In order to compare the calculation delays (complexity) of the proposed and conventional FCS–MPCC algorithms, the execution time is tested offline by using the code execution time measurement function of the processor (with an emulator). Fig. 4 shows the experimental results of the traditional and the new methods without compensation. At first, it can be seen both algorithms show remarkable dynamics over the low and medium speed range. Specifically, the settling time (from 0 to 350 r/min) is shorter than 0.1 s and the system shows strong robustness against the external load disturbance. Whereas, when the machine is controlled to approach the rated point, although the rising time for the two methods is similar, the settling time for the new strategy is slightly longer (around 0.7 s) from the perspective of torque, and after 2.7 s, the torque ripples (TR) witness a visible decline. Then, the steady-state control performance of the two methods is different, which is mainly reflected in the d-axis current ripples (CDR), q-axis current ripples (CQR), and TR. First, the CDR, CQR, and TR of the traditional method are 3 A, 4 A, and 2.5 N·m under the no-load condition at 350 r/min, respectively. While they decrease by around 0.3 A (10%), 0.6 A (15%), and 0.5 N·m (16%) when the new algorithm is applied. Moreover, the same trend can be witnessed under load conditions. The CDR, CQR, and TR drop from 12 A, 6 A, and 3.5 N·m for the traditional discretization method to 11.5 A, 5.7 A, and 3.3 N·m for the proposed PPM. These represent that the novel method can improve the steady-state control performance in the LCF conditions. Finally, the execution delay time for the novel and traditional methods are 0.0327 and 0.0302 ms, respectively, proving that the computation complexity of the proposed FCS–MPCC method is slightly higher than that of the traditional one (as in Chapter II).

TABLE I
TIME DELAY IN 15 DIFFERENT PERIODS

kth period	Delay (ms)	kth period	Delay (ms)	kth period	Delay (ms)
1	0.0312	6	0.0328	11	0.0312
2	0.0322	7	0.0322	12	0.0326
3	0.0310	8	0.0313	13	0.0322
4	0.0325	9	0.0318	14	0.0322
5	0.0312	10	0.0326	15	0.0326

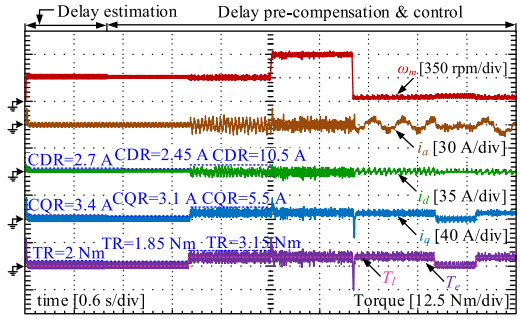

Fig. 5. Experimental results of the proposed strategy considering calculation delay compensation at control frequency of 2 kHz.

On the other hand, in order to verify the effectiveness of the brand-new online delay compensation strategy. The experimental setup is designed as follows: the machine is controlled by the new approach without compensation between 0 and 1 s, in which the delay time is estimated. Then, after 1 s, the proposed method with delay compensation is adopted for control. First, Table I records the estimated calculation delay (containing sampling consumption) in 15 control periods. It can be seen that the differences among those data are small (maximum error is 0.0018 ms), so the assumption in Chapter III is reasonable. Besides, the average delay time can be calculated as 0.0320 ms, being very close to the offline test value. Then, Fig. 5 shows that under the no-load conditions, the CDR, CQR, and TR get down to 2.45 A, 3.1 A, and 1.85 N·m when the calculation delay algorithm is implemented. Moreover, in comparison with Fig. 4(b), the control ripples for the integrated method also experience a slight decrease (4.3% CDR, 3.5% CQR, and 4.5% TR) when the rated load is applied. In order to verify the effectiveness of the proposed delay compensation strategy more intuitively, Fig. 6 compares the steady-state performance before and after delay compensation when the machine operates at the rated point. Same as the results over the medium-speed range, the CDR,

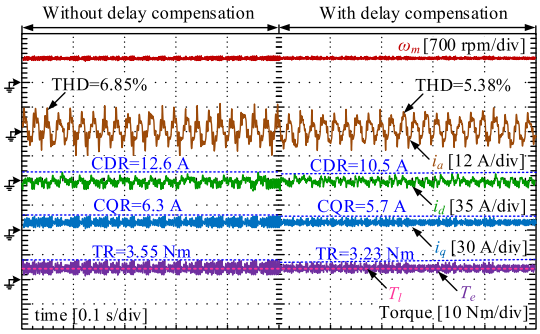

Fig. 6. Comparison of control performance before and after calculation delay compensation at control frequency of 2 kHz.

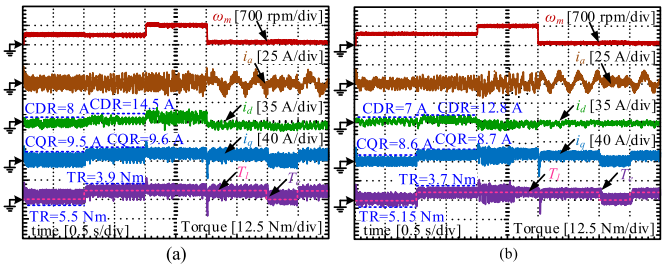

Fig. 7. Experimental results at control frequency of 1 kHz. (a) FCS–MPCC based on Euler discretization method. (b) FCS–MPCC based on proposed prediction plant without delay compensation.

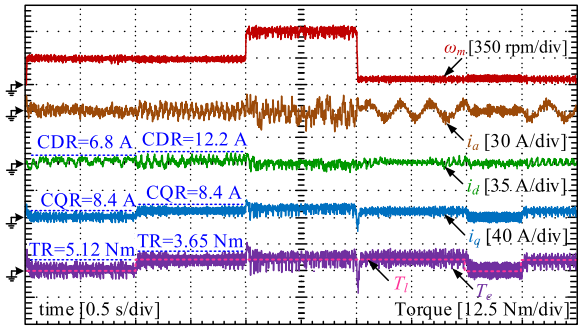

Fig. 8. Experimental results of the proposed strategy considering calculation delay compensation at control frequency of 1 kHz.

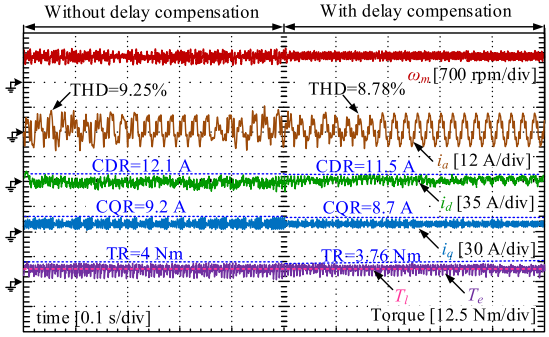

Fig. 9. Comparison of control performance before and after calculation delay compensation at control frequency of 1 kHz.

CQR, and TR experience a visible decline as well. Besides, the total harmonic distortion (THD) of phase current before delay compensation is 6.85%, which is about 27.3% higher than that after delay compensation. These verify that the delay compensation strategy is capable of reducing the current and TR so as to enhance the performance of the proposed FCS–MPCC strategy at the control frequency of 2 kHz.

B. Test Results at 1 kHz

Since that the calculation delay time has been illustrated previously, this part will directly compare the system performance among the traditional Euler discretization-based FCS-PCC, the proposed numerical solution-based FCS-MPCC without delay compensation and the proposed method with delay compensation. The experimental setups are consistent with the abovementioned ones. Fig. 7 illustrates the comparison results of the traditional and the proposed method without delay compensation. First, in comparison with the results at the control frequency of 2 kHz, the CDR, CQR, and TR become much larger regardless of the working conditions. Second, similar to Fig. 4, the proposed FCS–MPCC shows better steady-state performance than the traditional approach. In detail, the CDR, CQR, and TR of the traditional method are 8 A, 9.5 A, and 5.5 N·m under the no-load condition at 350 r/min, respectively, while they decrease to 7 A, 8.6 A, and 5.15 N·m when the new strategy is applied. And the same trend occurs for the load conditions. Fig. 8 demonstrates the experimental results of the proposed strategy with calculation delay compensation. Under the no-load condition at 350 r/min, the CDR, CQR, and TR are further smaller than those in Fig. 7(b), with the values of 6.8 A, 8.4 A, and 5.12 N·m, respectively. Compared to the results at the control frequency of 2 kHz, it can be seen that when the control frequency is lower, the delay compensation effect will get relatively less significant because the LCF contributes more to the system performance degradation. In Fig. 9, the steady-state performance of the proposed method without and with delay compensation at the rated point is compared. The THD of the phase current between 0 and 0.5 s is 9.25% and it drops to 8.78% between 0.5 and 1 s. Besides, similar to the results in Fig. 6, the ripples of d-, q-axis currents and torque get smaller after compensation as well.

V. Conclusion

This letter presents an accurate FCS–MPCC algorithm to improve the control performance of the surface-mounted PMSM used in the LCF cases. The contributions of this study are mainly reflected in the following two aspects. First, an accurate machine PPM based on numerical solutions is proposed to eliminate the diverse side effects caused by the traditional linear Euler discretization algorithm. By using the novel model, the precise future states can be calculated, ensuring that the optimal control voltage can be selected precisely. Second, instead of using the traditional calculation delay compensation method, a specially

designed compensation technique based on delay estimation and current precompensation is investigated. The experimental results demonstrate that the proposed FCS–MPCC algorithms are able to provide better steady-state performance than the traditional scheme under the LCF (with the control frequencies of both 1 and 2 kHz) situations. Meanwhile, the new method still shows remarkable dynamic control performance.

REFERENCES

[1] Z. Q. Zhu and Y. Liu, "Analysis of air-gap field modulation and magnetic gearing effect in fractional-slot concentrated-winding permanent-magnet synchronous machines," *IEEE Trans. Ind. Electron.*, vol. 65, no. 5, pp. 3688–3698, May 2018.

[2] J. Lu, X. Zhang, Y. Hu, J. Liu, C. Gan, and Z. Wang, "Independent phase current reconstruction strategy for IPMSM sensorless control without using null switching states," *IEEE Trans. Ind. Electron.*, vol. 65, no. 6, pp. 4492–4502, Jun. 2018.

[3] C. Gong, Y. Hu, G. Chen, H. Wen, Z. Wang, and K. Ni, "A DC-Bus capacitor discharge strategy for PMSM drive system with large inertia and small system safe current in EVs," *IEEE Trans. Ind. Inform.*, vol. 15, no. 8, pp. 4709–4718, Aug. 2019.

[4] X. Zhang, L. Zhang, and Y. Zhang, "Model predictive current control for PMSM drives with parameter robustness improvement," *IEEE Trans. Power Electron.*, vol. 34, no. 2, pp. 1645–1657, Feb. 2019.

[5] J. Liu, C. Gong, Z. Han, and H. Yu, "IPMSM model predictive control in flux-weakening operation using an improved algorithm," *IEEE Trans. Ind. Electron.*, vol. 65, no. 12, pp. 9378–9387, Dec. 2018.

[6] Y. Zhang, B. Xia, and H. Yang, "Performance evaluation of an improved model predictive control with field oriented control as a benchmark," *IET Electr. Power App.*, vol. 11, no. 5, pp. 677–687, 2017.

[7] S. Zhao, X. Huang, Y. Fang, and J. Zhang, "Compensation of DC-Link voltage fluctuation for railway traction PMSM in multiple low-switching-frequency synchronous space vector modulation modes," *IEEE Trans. Veh. Technol.*, vol. 67, no. 1, pp. 235–250, Jan. 2018.

[8] Z. Wang, B. Wu, D. Xu, and N. R. Zargari, "A current-source-converter-based high-power high-speed PMSM drive with 420-Hz switching frequency," *IEEE Trans. Ind. Electron.*, vol. 59, no. 7, pp. 2970–2981, Jul. 2012.

[9] Y. Wang *et al.*, "Deadbeat model-predictive torque control with discrete space-vector modulation for PMSM drives," *IEEE Trans. Ind. Electron.*, vol. 64, no. 5, pp. 3537–3547, May 2017.

[10] P. Cortes, J. Rodriguez, C. Silva, and A. Flores, "Delay Compensation in model predictive current control of a three-phase inverter," *IEEE Trans. Ind. Electron.*, vol. 59, no. 2, pp. 1323–1325, Feb. 2012.

[11] Y. Yang, H. Wen, and D. Li, "A fast and fixed switching frequency model predictive control with delay compensation for three-phase inverters," *IEEE Access*, vol. 5, pp. 17904–17913, 2017.

[12] X. Xiao, Y. Zhang, J. Wang, and H. Du, "An improved model predictive control scheme for the PWM rectifier-inverter system based on power-balancing mechanism," *IEEE Trans. Ind. Electron.*, vol. 63, no. 8, pp. 5197–5208, Aug. 2016.